

1 Development of a ddPCR approach for the absolute quantification of 2 soil microorganisms involved in atmospheric CO₂ fixation

4 Marie Le Geay^{1*} (marie.le-geay@univ-tlse3.fr), Kyle Mayers² (kyma@norceresearch.no), Martin
5 Küttim³ (kyttim@tlu.ee), Béatrice Lauga⁴ (beatrice.lauga@univ-pau.fr), and Vincent E.J. Jassey¹
6 (vincent.jassey@univ-tlse3.fr)

7
8 ¹ Centre de Recherche sur la Biodiversité et l'Environnement (CRBE), Université de Toulouse,
9 CNRE, IRD, Toulouse INP, Université Toulouse 3 – Paul Sabatier (UT3), Toulouse, France

10 ² Molecular Ecology and Paleogenomics - MEP, NORCE, Bergen, Norway

11 ³ Institute of Ecology, School of Natural Sciences and Health, Tallinn University, Uus-Sadama 5,
12 Tallinn, Estonia

13 ⁴ Université de Pau et des Pays de l'Adour, E2S UPPA, CNRS, IPREM, Pau, France

14
15 *corresponding authors: marie.le-geay@univ-tlse3.fr and vincent.jassey@univ-tlse3.fr

16
17 **Running title:** Quantification of CO₂ fixing microbes abundance

18
19 **Author contributions**

20 MLG, BL and VEJJ conceived the study. VEJJ collected the samples in each site with the help of
21 MK. MLG analyzed the samples with the help of BL and KM. MLG performed the statistical
22 analyses. MLG wrote the first draft of the manuscript with the help of BL and VEJJ. All co-authors
23 reviewed and contributed to the final form of the manuscript.

24
25 **Data availability**

26 Data related to this paper will be available from Figshare (10.xxxx/m9.figshare.c.xxxx) upon
27 publication.

28
29 **Conflict of interest**

30 The authors declare no conflict of interest.

32 **Abstract**

33 Carbon fixing microorganisms (CFMs) play a crucial role in soil carbon (C) cycling contributing to
34 carbon uptake and sequestration through various metabolic pathways. Despite their significance,
35 quantification of the absolute abundance of CFMs in soils remains elusive. This study employed
36 a digital droplet PCR (ddPCR) approach to quantify the abundance of key and emerging CFM
37 pathways in fen and bog across different depths (0-15 cm). Targeting total prokaryotes (*16S rRNA*
38 gene), oxygenic phototrophs (*23S rRNA* gene), aerobic anoxygenic phototrophic bacteria
39 (AAnPB, *pufM* gene), and chemoautotrophs (*cbbL* gene), we optimized ddPCR conditions to
40 achieve absolute quantification of these genes. Overall, our results revealed that oxygenic
41 phototrophs were the most abundant CFMs, constituting 12% of total prokaryotic abundance,
42 followed by chemoautotrophs (10%) and AAnPBs (9%). Fen exhibited higher gene concentrations
43 than bog. Depth variations were also observed, differing between fen and bog for all genes. Our
44 findings highlight the abundance of oxygenic phototrophs and chemoautotrophs in peatlands,
45 challenging previous estimations that relied solely on oxygenic phototrophs for microbial CO₂
46 fixation assessments. Incorporating absolute gene quantification is crucial for a comprehensive
47 understanding of microbial contributions to soil processes, shedding light on the intricate
48 mechanisms of soil functioning in peatlands.

49

50 Keywords : ddPCR, absolute abundance, CO₂ fixation, peatlands, oxygenic phototrophs,
51 chemoautotrophs, aerobic anoxygenic phototrophic bacteria

52

53 Introduction

54 Carbon fixing microorganisms (CFMs) are key drivers of the carbon (C) cycle as they
55 assimilate atmospheric CO₂ and contribute to the soil organic C sequestration (Yuan et al., 2012;
56 Ge et al., 2013; Liu et al., 2018). CFMs fix CO₂ through six major metabolic pathways, namely,
57 the reductive pentose phosphate cycle (also known as Calvin-Benson-Bassham, CBB cycle), the
58 reductive citrate cycle (rTCA cycle), the 3-hydroxypropionate bi-cycle (3-HP cycle), the 3-
59 hydroxypropionate/4-hydroxybutyrate cycle (3-HP/4-HB cycle), the dicarboxylate-
60 hydroxybutyrate cycle (DC/4-HB cycle) and the reductive acetyl-CoA pathway (also known as
61 Wood-Ljungdahl pathway) (Liu et al., 2018; Huang et al., 2022). The CBB cycle is the predominant
62 pathway utilized by microorganisms in soils (Bay et al., 2021). It is present across different
63 taxonomic levels (bacteria and protists), notably in green algae, diatoms, cyanobacteria and
64 aerobic eubacteria (Berg, 2011; Yuan et al., 2012). Oxygenic phototrophs and chemoautotrophs
65 are two major CFMs using the CBB cycle to fix atmospheric CO₂. Oxygenic phototrophs derive
66 their energy from light to assimilate CO₂ through photosynthesis, whereas chemoautotrophs use
67 reduced chemical compounds such as sulfur compounds, molecular hydrogen and reduced
68 metals to assimilate CO₂ (Hügler and Sievert, 2011). Potential CO₂ fixation through the CBB cycle
69 also recently emerged in aerobic anoxygenic phototrophic bacteria (AAnPBs). Recent studies
70 found AAnPB strains possessing (and expressing) genes of the CBB cycle (Graham et al., 2018;
71 Tang et al., 2021). Even though CFMs are now well recognized for their role in autotrophic CO₂
72 fixation in soils, their absolute quantification remains elusive (Liao et al., 2023). As microbial CO₂
73 assimilation rates are closely linked to CFMs abundance (Hamard et al., 2021a, 2021b; Liao et
74 al., 2023), it is essential to provide absolute quantification of these microorganisms in soils to
75 better assess their contribution in C fixation in terrestrial ecosystems.

76 Absolute quantification of microorganisms can be laborious notably in complex matrices such
77 as soils. Numerous approaches are available with their own strengths and flaws (Xiaofan Wang

78 et al., 2021). Methods based on cells counts such as fluorescence microscopy or flow cytometry
79 have been widely used (Bressan et al., 2015; Frossard et al., 2016), as have methods based on
80 adenosine triphosphate quantification (Karl, 1980; Hammes et al., 2010) or phospholipids fatty
81 acids analysis (PLFA, Frostegård and Bååth, 1996). However, these methods (except PLFA) do
82 not allow differentiation between different bacterial groups. Since the development of Polymerase
83 Chain Reaction (PCR, Mullis et al., 1986), different molecular approaches, such as real-time PCR
84 (qPCR, Higuchi et al., 1993), digital PCR (dPCR, Vogelstein and Kinzler, 1999) and digital droplet
85 PCR (ddPCR, Hindson et al., 2011) have emerged to count either total bacteria (using primers
86 targeting the *16S rRNA* gene) or specific populations of bacteria and their associated functions
87 (using primers targeting specific genes; Fig. S1). qPCR is based on the monitoring of the
88 amplification after each PCR cycle by using a fluorescent probe (Higuchi et al., 1993; Pinheiro et
89 al., 2012; Hou et al., 2023). However, this method requires external calibration and normalization
90 with endogenous controls (Hindson et al., 2011). It is also sensitive to inhibitors and to the initial
91 amount of the target since low concentrations will hardly be detected (Hindson et al., 2011;
92 Pinheiro et al., 2012; Taylor et al., 2017; Hou et al., 2023). On the other hand, ddPCR does not
93 require external calibration or normalization. This method uses water-in-oil droplets allowing
94 single molecule amplification. Droplets can either contain the target molecule or not. After being
95 amplified with a fluorescent probe or labeling dye, it is possible to discriminate between positive
96 and negative droplets (see Hindson et al., 2011). Several studies have compared qPCR and
97 ddPCR and found that ddPCR had better precision, repeatability, sensitivity and stability than
98 qPCR (Zhao et al., 2016; Taylor et al., 2017; Xue et al., 2018; Wang et al., 2022). Nowadays,
99 ddPCR is increasingly used in environmental studies (see Hou et al., 2023 for a complete review),
100 even though several challenges are faced and require appropriate optimization of ddPCR
101 parameters (see Kokkoris et al., 2021). Adjusting many factors relating to the PCR reaction,
102 including concentration of template DNA, thermocycling conditions, and the threshold setting used

103 to discriminate positive and negative droplets can notably influence the detection of target DNA
104 from environmental samples (Witte et al., 2016; Rowlands et al., 2019; Kokkoris et al., 2021).

105 In this study, we aim to provide an absolute quantification of the main (oxygenic phototrophs
106 and chemoautotrophs) and emerging (AAnPBs) CFMs in peatlands. As peatlands are a major C
107 reservoir (Nichols and Peteet, 2019), quantifying the main CFMs will enhance our understanding
108 of peatland C cycling. More precisely, we aimed to (1) optimize ddPCR conditions to enumerate
109 total prokaryotes and specific groups of CFMs (oxygenic phototrophs, chemoautotrophs and
110 AAnPBs), (2) apply optimized ddPCR to target CFMs in two peatland types (moderately rich fen
111 and open bog) and (3) at different depths (0-15 cm). We hypothesized that oxygenic phototrophs,
112 who can be found within bacteria and protists, will be the most abundant CFMs in peatlands. We
113 also forecast that CFMs absolute abundance will differ between the bog and the fen as these two
114 peatland habitats harbor different biotic and abiotic factors. We further hypothesized that oxygenic
115 phototrophs and AAnPBs will be less abundant with depth as the amount of light decreases, thus
116 favoring chemoautotrophs.

117

118 **Experimental procedure**

119 **Sampling and DNA extraction**

120 Peat samples were collected in two peatlands, Counozouls (France) and Männikjärve (Estonia).
121 Counozouls mire is located in the French Pyrenees mountains (42°41'16"N - 2°14'18"E – 1.374
122 m a.s.l). It is a moderately rich fen belonging to the Special Area of the Natura 2000 Conservation
123 site "Massif du Madres Coronat". The peatland of Männikjärve is an open bog located in the Endla
124 mire system in Central Estonia (58°52'26.4"N - 26°15'03.6"E – 82 m a.s.l). At each site, we
125 collected three cores in similar and homogeneous habitat by cutting peat soil. Then, the cores
126 were cut into three depths corresponding to the living layer (D1; 0-5 cm), the decaying layer (D2;
127 5-10 cm), and the dead layer (D3; 10-15 cm). At each depth, few grams of peat were collected,
128 cut in small pieces, homogenized and placed in sterile 5 mL Eppendorf tubes containing 3 mL of
129 RNA/*later* (ThermoFisher). The tubes were stored at -20°C upon our arrival in the laboratory. DNA
130 was extracted using the DNeasy PowerSoil Pro Kit (Qiagen) following manufacturer's instructions.
131 After elution of DNA (70 µL in final solution), DNA concentration was quantified using a Nanodrop
132 ND-1000 spectrophotometer. Extracts were then stored at -20°C prior to DNA amplification.

133

134 **Primer choice and design**

135 Total concentration of prokaryotes was obtained by targeting the 16S *rRNA* gene. Microorganisms
136 involved in oxygenic photosynthesis were quantified using the 23S *rRNA* gene while
137 chemoautotrophs were quantified using the *cbbL* gene that encodes the large subunit of RubisCO
138 form IA (Kusian and Bowien, 1997; Alfreider and Bögensperger, 2018). We used the *pufM* gene
139 that encodes for the M subunit of type II photochemical reaction center to target AAnPBs
140 (Achenbach et al., 2001; Béjà et al., 2002). To select the primers, we first searched the literature
141 and identified primer pairs that have been already used either in ddPCR or in qPCR. We used the
142 primer pairs L/Prba338f and K/Prun518r for prokaryotes (Øvreås et al., 1997),

143 cbbLR1F/cbbLR1inR for chemoautotrophs (Selesi et al., 2007) and
144 pufMforward557/pufMreverse750 for AAnPBs (Table 1; Du et al., 2006). However, we could not
145 find suitable primers matching a short region of the 23S *rRNA* gene targeting oxygenic
146 phototrophs with satisfying length and degeneracies. Therefore, we designed a new set of primers
147 for ddPCR.

148 To do so, we first conducted a PCR on peat samples to target the 23S *rRNA* gene using
149 the existing primers P23SrV-f1 with P23SRV-r1 (Sherwood and Presting, 2007) and sequenced
150 PCR amplicons. The PCR program was run in a total volume of 50 μ L containing 25 μ L of
151 AmpliTaq GoldTM Master Mix (applied biosystem, ThermoFisher), 19 μ L of ultrapure water, 1 μ L
152 of forward and 1 μ L of reverse primer (final concentration of 20 μ M) and 2 μ L of DNA template.
153 The PCR reaction conditions were an initialization of 10 min at 95°C followed by 35 cycles of 1
154 min at 94°C, 45 s at 55°C, 45 s at 72°C and a final extension step of 10 min at 72°C. PCR quality
155 was assessed using 1.65% agarose gel electrophoresis. The high throughput sequencing was
156 performed by the GeT-PlaGe plateform (Genotoul, Toulouse, France) using Illumina MiSeq v3
157 technology. Based on the results of the sequencing we designed the new forward primer 23S255f
158 to target a short region of the 23S *rRNA* gene. We aligned all the sequences obtained from
159 sequencing using Clustal Omega (EMBL-EBI) and blasted (nBLAST with NCBI) these sequences
160 to ensure that they corresponded to the 23S *rRNA* gene. Then, using BioEdit v5.0.9 we generated
161 a consensus sequence based on the aligned sequences (Fig. S2). We searched in this consensus
162 sequence a conserved region and checked every degenerated base to create a manually curated
163 sequence. We examined if this sequence matched guidelines for q/dPCR (Rodríguez et al., 2015)
164 (amplicon length <250 pb, GC content of 50-60%, annealing temperature of 50-65°C, no
165 secondary structure and primer-dimer, no repetition of Gs and Cs longer than 3 bases, Table S1)
166 and finally obtained the new forward primer 23S255f: 5'- GGA TTA GAT ACC CYD GTA GTC C
167 -3'. By using the new primer set, the forward primer 23S255f with the reverse primer P23SRV-r1
168 (~160 pb), we targeted oxygenic phototrophs.

169 **ddPCR conditions**

170 Absolute abundance of genes was measured using digital droplet PCR (ddPCR, BioRad). The
171 ddPCR reactions were run in a total volume of 20 μL on a DX200 instrument (BioRad) with 10 μL
172 of EvaGreen Supermix (BioRad, 1X), 0.5 or 0.3 μL of each primer (final concentration 250 nM or
173 150 nM respectively) and 4 μL of ultrapure water. Template DNA (5 μL) diluted at 10, 100 or 1,000
174 times was added to the reaction mix. This mixture was then emulsified with QX200 Droplet
175 Generation Oil for EvaGreen (BioRad) using the QX200 Droplet Generator (BioRad) and was
176 manually transferred into a 96-well PCR plate. The plate was heat-sealed with a foil seal and then
177 placed on a C1000 Touch Thermocycler with deep-well module (BioRad) to run the PCR using
178 different programs (see section ‘*ddPCR optimization*’). Following amplification, plates were
179 equilibrated for at least 10 min at room temperature. Then, plates were loaded on a QX200 Droplet
180 Reader (BioRad) and the fluorescence was read and analyzed using QuantaSoft software.
181 Threshold for positive and negative droplets were manually defined using ultrapure water as a
182 negative control and DNA extracted from different cultures of microorganisms as positive and
183 negative controls. *Escherichia coli* DNA was used as a positive control for prokaryotes and as a
184 negative control for the other genes. *Micromonas pusilla* (a micro-algae) DNA was used as a
185 positive control for oxygenic phototrophs. QuantaSoft provides a final concentration of target
186 copies. μL^{-1} of ddPCR reaction. We first calculated the total concentration in 20 μL of ddPCR
187 reaction and normalized it by the weight of dry peat to obtain a final concentration in target
188 copies. g^{-1} of dry peat (copies. g^{-1} DW).

189

190 **ddPCR optimization**

191 For all the assays we tested two primer concentrations (150 nM and 250 nM); a temperature
192 gradient based on the theoretical annealing temperature of the primers; different dilution of the
193 template (1/10, 1/100 and 1/1,000) and different species DNA to find controls (*E. coli*, *M. pusilla*).

194 We defined thermocycling conditions as 98°C for 5 min followed by 40 cycles of 94°C for 30 s,
195 different temperature or gradient of temperature for 30 s, followed by 5 min at 4°C and 98°C for
196 10 min. The ramp rate was set up at 2°C/s . When required, these parameters were adjusted to
197 optimize the assays. For two assays (16S and 23S *rRNA* genes) we used the following PCR
198 conditions: 98°C for 5 min followed by 40 cycles of 94°C for 30 s, 61°C and 57.6°C for 1 min,
199 followed by 5 minutes at 4°C and 98°C for 10 min with a ramp rate stetted up at 2°C/s and for the
200 others (*cbbL* and *pufM* genes) we used: 98°C for 5 min followed by 45 cycles of 94°C for 1 min,
201 53°C and 50.2°C for 2 min, followed by 5 min at 4°C and 98°C for 10 min with a ramp rate stetted
202 up at 1°C/s (Table 2).

203

204 **Statistical analysis**

205 Data were visually checked and tested for normality and homoscedasticity, and log-transformed
206 when necessary. Normality was assessed using Shapiro-Wilk test (Shapiro and Wilk, 1965). In
207 order to see if the genes concentrations differed according to location or depth we conducted a
208 one-way ANOVA. We also tested if the concentration significantly differed according to the gene
209 targeted. Post-hoc test (Tukey honestly significant difference test) was further applied when a
210 significant difference was found between location, depth and genes (Keselman and Rogan, 1977).
211 Statistical analyses were performed using RStudio v12.0 (RStudio Team, 2020) and graphical
212 representations were done using ggplot2 v3.4.0 (Wickham, 2016).

213

214

215

216

217

218 **Results and Discussion**

219 **Optimized ddPCR succeed to amplify universal and specific genes from peat** 220 **samples**

221 We tested different ddPCR conditions to obtain both a good amplification of the target genes and
222 a separation between positive and negative clouds of droplets (Fig. 1). When numerous droplets
223 were present without a clear separation (rain), ddPCR conditions were optimized (Fig. S3-S6)
224 following recommendations from previous studies (Witte et al., 2016; Rowlands et al., 2019;
225 Kokkoris et al., 2021). We notably optimized the primers annealing temperature (better separation
226 of the droplets), the dilution of the target (dilution of potential inhibitors and avoid saturation of the
227 target, Fig. S3 well A05), the thermocycling conditions (denaturation/annealing/elongation times,
228 number of cycle and ramp rate leading to compacts clouds of positive and negative droplets well
229 separated) and we used positive and negative controls to set an appropriate thresholds (Witte et
230 al., 2016; Rowlands et al., 2019; Demeke et al., 2021; Kokkoris et al., 2021). Results of the
231 optimization are presented in Table 2 and Supplementary Figures S3, S4, S5 and S6.

232 Once the assays were otpimised, we used the ddPCR parameters defined to amplify DNA
233 from samples of the two peatlands location (Table 2). We retrieved 16S rRNA gene
234 concentrations of $10.3 \pm 2.76 \times 10^6$ copies.g⁻¹ DW in Counozouls and $2.11 \pm 0.21 \times 10^6$ copies.g⁻¹
235 DW in Männikjärve. Previous peatlands studies found total bacterial concentrations from 1×10^6
236 copies.g⁻¹ DW or copies.mL⁻¹ (Gilbert et al., 1998; Lew et al., 2016) to 1×10^{10} copies.g⁻¹ DW or
237 copies.mL⁻¹ (Lin et al., 2012; Wen et al., 2018) which is consistent with our findings. Our data
238 further showed that CFMs genes concentrations were very similar ($P > 0.05$, ANOVAs; Fig. 2).
239 Average 23S rRNA gene concentration was $14.0 \pm 2.62 \times 10^5$ copies.g⁻¹ DW in Counozouls and
240 $6.98 \pm 1.67 \times 10^5$ copies.g⁻¹ DW in Männikjärve. Again, this is consistent with other findings from
241 soils (Jassey et al., 2022) and in particular peatlands where concentrations around $1 \times 10^5 - 10^6$
242 copies.g⁻¹ DW have been found using microscopy and qPCR (Gilbert et al., 1998; Jassey et al.,

243 2015; Reczuga et al., 2018; Tang et al., 2018). On average, *cbbL* gene concentration was $9.90 \pm$
244 2.36×10^5 copies.g $^{-1}$ DW in Counozouls and $2.57 \pm 0.43 \times 10^5$ copies.g $^{-1}$ DW in Männikjärve.
245 Similar abundances were retrieved in soils using qPCR (Xiao et al., 2014; Keshri et al., 2015;
246 Xiayu Wang et al., 2021; Yin et al., 2022). For the *pufM* gene, $8.17 \pm 1.59 \times 10^5$ copies.g $^{-1}$ DW
247 were retrieved in Counozouls and $3.24 \pm 0.61 \times 10^5$ copies.g $^{-1}$ DW in Männikjärve. Again, these
248 concentrations were comparable to AAnPBs concentrations found in soils ($1-50 \times 10^5$ copies.g $^{-1}$)
249 or in aquatic environments ($6 \times 10^4 - 12 \times 10^5$ copies.mL $^{-1}$) (Lew et al., 2016; Sato-Takabe et al.,
250 2016, 2020; Tang et al., 2018). All together, these results showed that ddPCR is a suitable and
251 reliable method to quantify absolute gene concentrations from complex soil matrices, like peat.
252 Indeed, peat samples are usually rich in humic substances that are hardly removed during DNA
253 extraction (Delarue et al., 2011). Their presence in DNA sample can inhibit Taq DNA polymerase
254 and the fluorescence signal of double-stranded DNA binding dyes (Sidstedt et al., 2015). By
255 optimizing ddPCR parameters we were able to overcome this issue and improve the separation
256 between positive and negative droplets.

257

258 **The abundance of CFMs differ between fen and bog and with depth**

259 Overall, we found that gene concentrations in the fen were up to 4 times greater than gene
260 concentrations in the bog ($P < 0.05$ for all genes, ANOVAs; Fig. 2). This pattern agrees with
261 previous findings on total bacteria (Lin et al., 2012; Mpamah et al., 2017; Xu et al., 2021) and
262 photoautotrophic bacteria (Hamard et al., 2021a; Sytiuk et al., 2022) abundances assessed by
263 either inverted microscopy, flow cytometry or PLFA assays. As a moderately rich fen and an open
264 bog, Counozouls and Männikjärve present different nutrient contents, acidity and vegetation cover
265 (Sytiuk et al., 2022) suggesting that these conditions are strong determinants of CFM abundance
266 in peatlands. This finding corroborates previous findings on microbial CO $_2$ fixation in soils, where
267 nutrient and water content (Guo et al., 2015; Zhao et al., 2021), soil pH and soil organic carbon
268 (SOC) (Lin et al., 2012; Nowak et al., 2015; Lew et al., 2016; Zhao et al., 2021) have been shown

269 to influence microbial abundance in general and microbial CO₂ fixation in particular. Additionally,
270 or alternatively, our data also suggest that climate may determine CFM abundances. Counozouls
271 and Männikjärve are located at different latitudes, and thus harbor different climate with warmer
272 and wetter conditions in Counozouls than in Männikjärve (Sytiuk et al., 2022). Thus, warmer and
273 wetter conditions in Counozouls may have increased the abundance of CFMs as previously
274 shown for peatlands microbes (Le Geay et al., 2024), but also for microbial biomass in soils (Yuan
275 et al., 2012; Xu et al., 2013). Although the exact environmental drivers of CFM abundance in
276 peatlands still need to be identified, our results suggest that complex interactions between
277 climate, peat properties and vegetation cover might determine CFM abundance in peatlands.
278 Alternatively, DNA found in peat can be a mix of DNA from active cells, dead cells or even
279 extracellular DNA (Pearman et al., 2022), which could explain the observed high abundance in
280 the fen. Physicochemical conditions found in Counozouls may better preserve the DNA letting
281 both active and dead cells preserved. More site comparisons will be required in the future to
282 further understand this observed pattern.

283 In addition to peatland type effect, our data evidenced a net depth effect but with opposite
284 patterns between the fen and the bog (Fig. 3). In Counozouls, all gene concentrations aside from
285 23S rRNA and *pufM* increased ($P < 0.05$, ANOVAs; Fig. 3; Tables S2-S5) while in Männikjärve,
286 all gene concentrations but 16S rRNA decreased with depth ($P < 0.05$, ANOVAs; Fig. 3; Tables
287 S2-S5). More particularly, we found that the concentration of the 23S rRNA gene did not vary with
288 depth ($P > 0.05$) except between D2 and D3 samples in Counozouls ($P < 0.05$; Fig. 3; Table S3),
289 while it gradually decreased with depth in Männikjärve ($P < 0.001$; Fig. 3; Table S3). As oxygenic
290 phototrophs biomass is tightly linked to light availability (Bengtsson et al., 2018), we were
291 expecting such a decrease of the 23S rRNA gene with depth. We tentatively explain the high
292 abundance of the 23S rRNA gene with depth in Counozouls by the dominance of cyanobacteria
293 in the oxygenic phototrophic community (Fig. S7). Indeed, cyanobacteria can capture light at low

294 intensities thanks to highly adaptable eco-physiological traits (Carey et al., 2012) and could
295 therefore remain abundant with depths in Counozouls.

296 Concentration of the *cbbL* gene targeting chemoautotrophs significantly increased with
297 depth in Counozouls ($P < 0.05$, ANOVA) whereas it significantly decreased with depth in
298 Männikjärve ($P < 0.001$; ANOVA; Fig. 3; Table S4). Chemoautotrophs are notably studied in deep
299 sea vents, coastal sediments, and soils, where reduced compounds such as sulfur compounds,
300 molecular hydrogen and reduced metals are particularly abundant and facilitate chemoautotrophy
301 (Nakagawa and Takai, 2008; Boschker et al., 2014; Gomez-Saez et al., 2017; Yang et al., 2017;
302 Wang et al., 2023). Usually chemoautotrophs are active in the first centimeters of coastal
303 sediments as conditions are limiting in the deeper layers. We retrieved such a pattern in
304 Männikjärve but not in Counozouls, suggesting that geochemical conditions for chemoautotrophs
305 might be less limiting in Counozouls. For the *pufM* gene that targets AAnPBs, we did not see a
306 significant difference in gene concentrations between depth in Counozouls ($P > 0.05$). In
307 Männikjärve we found a significant decrease of the *pufM* gene concentration with depth ($P <$
308 0.001; ANOVA; Fig. 3; Table S5). Being obligate aerobic microorganisms, AAnPBs have mainly
309 been found in the euphotic zone of aquatic systems (Koblížek et al., 2003). They are often
310 described as highly active part of microbial communities; however, we are lacking information
311 regarding their importance in soil communities as well as their metabolic capacities with only a
312 few studies working on AAnPBs in soils (Feng et al., 2011; Tang et al., 2018). Our data show that
313 AAnPBs are more abundant in fens than in bogs, suggesting they could play an important
314 ecological role in these ecosystems.

315

316 **Ratios of oxygenic phototrophs, chemoautotrophs and AAnPBs compared to total**
317 **prokaryotes reveals their equally importance in peatlands**

318 Our data revealed that compared to total prokaryotes, prokaryotic oxygenic phototrophs,
319 chemoautotrophs and AAnPBs were equally abundant. Prokaryotic oxygenic phototrophs and
320 chemoautotrophs represented ~8% and ~10% of total prokaryotes in Counozouls and ~16% and
321 ~10% in Männikjärve. These results showed that chemoautotrophs were more or less as
322 abundant as oxygenic phototrophs, and possibly equally contributed to CO₂ fixation in peatlands.
323 This contradicts the first estimates of phototrophic and chemoautotrophic CO₂ fixation rates in
324 peatlands showing that chemoautotrophic CO₂ assimilation represented less than 1% of oxygenic
325 phototrophic CO₂ fixation (Gilbert et al. 1998). Further work quantifying chemoautotrophic CO₂
326 fixation in peatlands will be necessary in the future. Also, the use of RNA quantification instead of
327 DNA may better evidence abundance patterns between phototrophs and chemoautotrophs.
328 Furthermore, our results show that AAnPBs represented ~8% of total prokaryotes in Counozouls
329 and ~15% of total prokaryotes in Männikjärve, suggesting they may play a significant role in the
330 C cycle of peatlands as some strains possessing CBB cycle genes can actively fix atmospheric
331 CO₂ (Graham et al., 2018; Tang et al., 2021). Altogether these results show that further work is
332 urgently needed to better quantify the contribution of microorganisms to peatland CO₂ uptake as
333 current estimates based on sole oxygenic phototrophs (Hamard et al., 2021a) may be strongly
334 underestimated. Soils are also facing important climate and land use changes which can
335 profoundly affect soil microbiomes and their functions (Solomon et al., 2007; Lode et al., 2017;
336 IPCC, 2023). Changing soil microbiome can notably impact C fixation and emission (Blankinship
337 et al., 2011; Zhou et al., 2020; Li et al., 2022; Le Geay et al., 2024). These changes could lead to
338 enhanced microbial CO₂ fixation in some soils, which could mitigate global changes (Qiu et al.,
339 2020; Strack et al., 2022; Le Geay et al., 2024). Therefore, knowing the contribution of the different
340 CFMs and their metabolic pathway to soil microbial CO₂ fixation is also a key forecast about the
341 changes in soils C cycle.

342

343 To conclude, this study evidenced that ddPCR can be optimized to amplify targets coming
344 from a complex matrix such as peat and can be used to target both universal markers (*16S rRNA*
345 gene) and specific markers (e.g., *23S rRNA*, *cbbL* or *pufM* genes). Taken together, the results of
346 this study support the effective use of ddPCR to analyze target gene concentrations in different
347 peatland types and at different depths. These results further highlight a complicated picture in
348 which major and emerging CFMs may all play a key role in peatland microbial CO₂ fixation. This
349 requires further support in the future to better understand peatland C cycle. Using a cutting-edge
350 method such as ddPCR can therefore help to better understand the relevance and contribution of
351 CFMs for the soil C cycle. Absolute quantification, which simplifies the quantification of functional
352 genes, provides a better understanding of microbial ecology and its underlying processes within
353 the ecosystems functioning.

354

355 **Acknowledgements**

356 This work has been supported by the MIXOPEAT (Grant No. ANR-17-CE01-0007 to VEJJ) and
357 BALANCE (Grant No. ANR-23-ERCC-0001-01) projects funded by the French National Research
358 Agency. This study has been partially supported through the grant EUR TESS N°ANR-18-EURE-
359 0018 in the framework of the Programme des Investissements d'Avenir.

360

361 **Tables**

362 **Table 1.** Primer pairs used in this study

Microorganisms targeted	Primers	Amplicon Size	Primer sequence	Reference
Prokaryotes	L/Prba338f	180 bp	5'- ACT CCT ACG GGA GGC AGC AG -3'	(Øvreås et al., 1997)
	K/Prun518r		5'- ATT ACC GCG GCT GCT GG -3'	
Oxygenic phototrophs	23S255f	160 bp	5'- GGA TTA GAT ACC CYD GTA GTC C -3'	This study
	P23Srv_r1		5'- TCA GCC TGT TAT CCC TAG AG -3'	(Sherwood and Presting, 2007)
Chemoautotrophs	cbbLR1F	274 bp	5'- AAG GAY GAC GAG AAC ATC -3'	(Selesi et al., 2007)
	cbbLRintR		5'- TGC AGS ATC ATG TCR TT -3'	
AAnPBs	pufM forward 557	193 bp	5'-TAC GGS AAC CTG TWC TAC-3'	(Du et al., 2006)
	pufM reverse 750		5'-CCA TSG TCC AGC GCC AGA A-3'	

363

364 **Table 2. Optimized ddPCR parameters** including primers concentration, DNA template dilution, optimal annealing temperature, ddPCR thermocycling conditions and positive and negative controls, UPW = ultra-pure water

Primers	L/Prba338f with K/Prun518r	23S255f/ P23Srv-r1	cbbLR1F/ cbbLRintR1	pufMfwd557/ pufMrev750
Gene targeted	16S rRNA	23S rRNA	cbbL	pufM
Primers concentration	150 nM	250 nM	250 nM	250 nM
DNA dilution	1/1,000	1/100 (D1, D2) and 1/10 (D3)	1/10	1/100 (D1, D2) and 1/10 (D3)
Annealing temperature	61 °C	57.6°C	53°C	50.2°C
ddPCR conditions	98°C – 5 min 40 cycles : 94°C – 30 s 61°C – 1 min	98°C – 5 min 40 cycles : 94°C – 30 s 57.6°C – 1 min	98°C – 5 min 45 cycles : 94°C – 1 min 53°C – 2 min	98°C – 5 min 45 cycles : 94°C – 1 min 50.2°C – 2 min

	4°C – 5 min 98°C – 10 min Ramp rate = 2°C/s	4°C – 5 min 98°C – 10 min Ramp rate = 2°C/s	4°C – 5 min 98°C – 10 min Ramp rate = 1°C/s	4°C – 5 min 98°C – 10 min Ramp rate = 1°C/s
Positive control	<i>E. coli</i> DNA	<i>M. pusilla</i> DNA	/	/
Negative control	UPW	<i>E. coli</i> DNA UPW	<i>E. coli</i> DNA UPW	<i>E. coli</i> DNA UPW

367

368

369 **Figure caption**

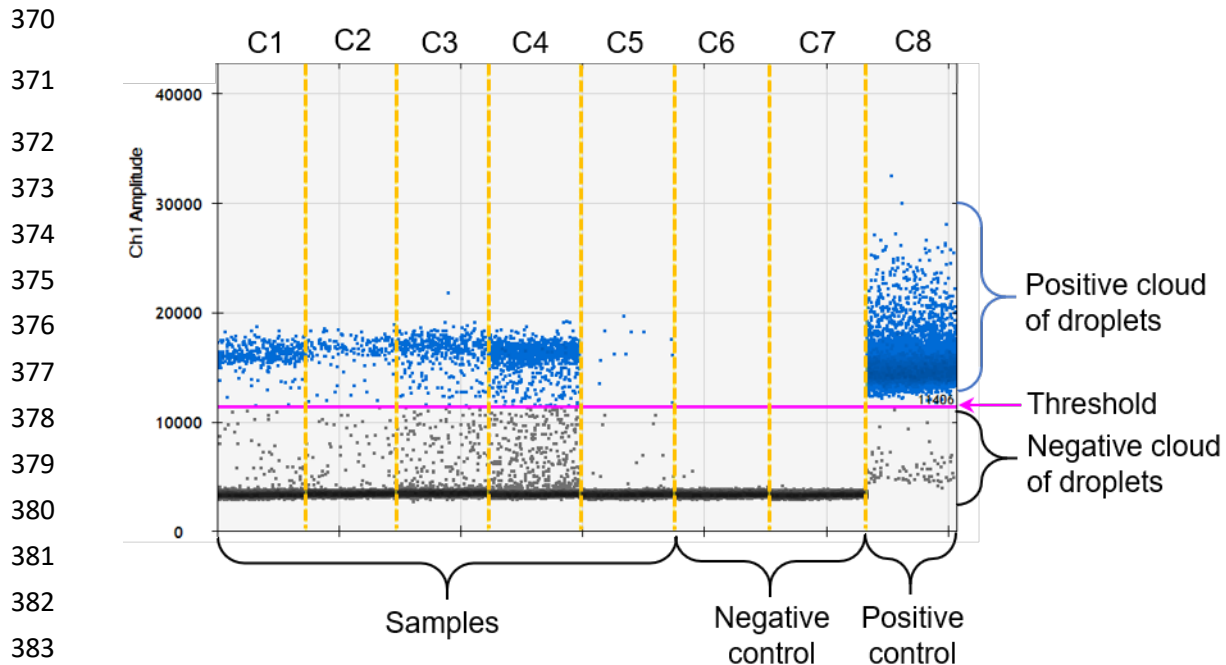


Figure 1. Example of results of ddPCR obtained for the 23S rRNA gene after analysis of raw data with QuantaSoft software. C1 to C5 = soil samples, C6 = ultrapure water (negative control), C7 = *E. coli* DNA (corresponding here to a negative control) and C8 = *M. pusilla* DNA (positive control). Horizontal purple line corresponds to the threshold manually set thanks to negative and positive controls. Blue dots correspond to positive droplets (containing target DNA) and black dots to negative droplets (not containing target DNA).

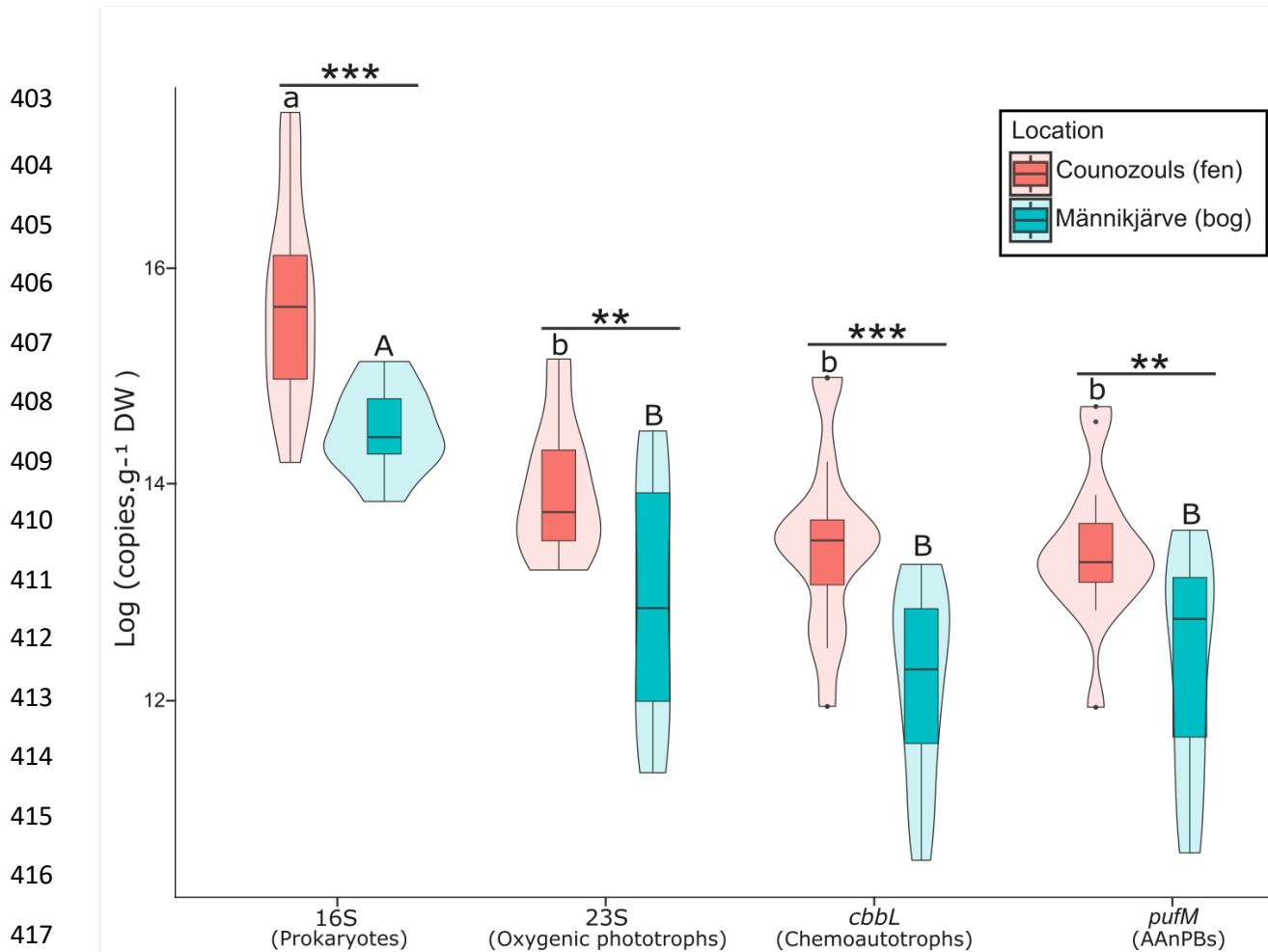


Figure 2. Absolute quantification of 16S rRNA gene targeting prokaryotes, 23S rRNA gene targeting oxygenic phototrophs, *cbbL* targeting chemoautotrophs and *pufM* targeting AAnPBs (all depth confounds) in Counozouls (fen) and Männikjärve (bog). Boxplots represent the logarithm of the total genes' copies.g⁻¹ DW and violin plots show the shape of data distribution. The horizontal black line in the box corresponds to the median and the edges of the box to 1st and 3rd quartiles. The vertical black line on the top and bottom of the boxplot represent respectively the highest and lowest values in the ± 1.5 interquartile range. Black dots correspond to the outliers. Lowercase and uppercase letters represent the difference between genes in Counozouls and Männikjärve, respectively. Horizontal bars with * represent the difference between peatlands (Counozouls and Männikjärve) for each gene, ** = $p < 0.01$; *** = $p < 0.001$. n = 15 for each gene at each location.

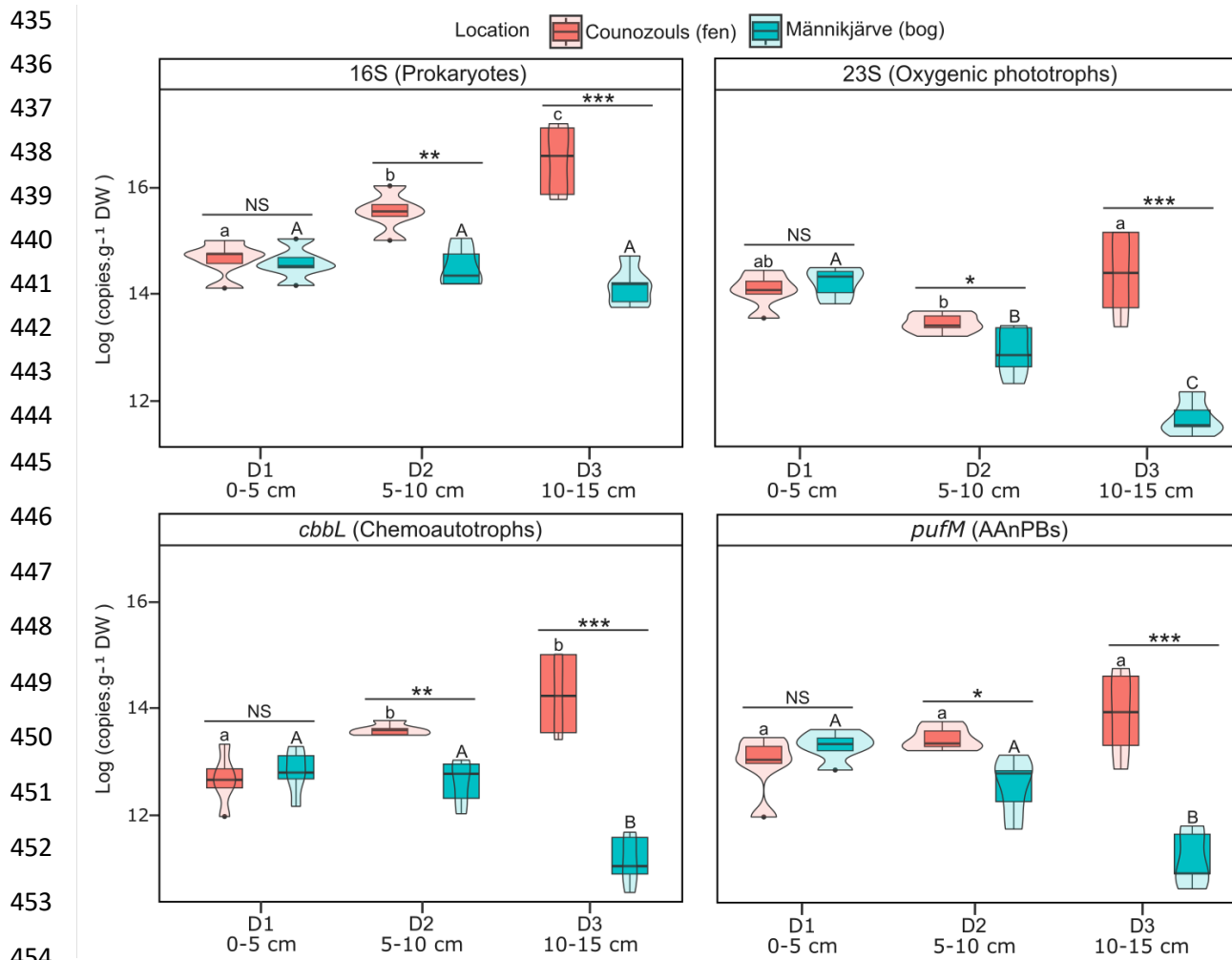


Figure 3. Absolute quantification of 16S rRNA gene targeting prokaryotes, 23S rRNA gene targeting oxygenic phototrophs, *cbbL* targeting chemoautotrophs and *pufM* targeting AAnPBs at different depths in Counozouls (fen) and Männikjärve (bog). Boxplots represent the logarithm of the total genes' copies.g⁻¹ DW and violin plots show the shape of data distribution. The black line in the box corresponds to the median and the edges of the box to 1st and 3rd quartiles. The vertical black line on the top and bottom of the boxplot represent respectively the highest and lowest values in the ± 1.5 interquartile range. Black dots correspond to the outliers. Lowercase and uppercase letters represent the difference between genes in Counozouls and Männikjärve, respectively. Horizontal bars with * represent the difference between peatlands (Counozouls and Männikjärve) at each depth. NS = not significant ($p > 0.05$); * = $p < 0.05$; ** = $p < 0.01$; *** = $p < 0.001$. n = 5 for each microbial group at each depth for each location. D1 (0-5 cm) corresponds to the living layer, D2 (5-10 cm) to the decaying layer and D3 (10-15 cm) to the dead layer.

468 Reference

469 Achenbach, L.A., Carey, J., Madigan, M.T., 2001. Photosynthetic and Phylogenetic Primers for Detection
470 of Anoxygenic Phototrophs in Natural Environments. *Applied and Environmental Microbiology* 67,
471 2922. doi:10.1128/AEM.67.7.2922-2926.2001

472 Alfreider, A., Bogensperger, T., 2018. Specific detection of form IA rubisCO genes in chemoautotrophic
473 bacteria. *Journal of Basic Microbiology* 58, 712–716. doi:10.1002/JOBM.201800136

474 Bay, S.K., Dong, X., Bradley, J.A., Leung, P.M., Grinter, R., Jirapanjawat, T., Arndt, S.K., Cook, P.L.M.,
475 LaRowe, D.E., Nauer, P.A., Chiri, E., Greening, C., 2021. Trace gas oxidizers are widespread and
476 active members of soil microbial communities. *Nature Microbiology* 2021 6:2 6, 246–256.
477 doi:10.1038/s41564-020-00811-w

478 Béjà, O., Suzuki, M.T., Heidelberg, J.F., Nelson, W.C., Preston, C.M., Hamada, T., Eisen, J.A., Fraser, C.M.,
479 DeLong, E.F., 2002. Unsuspected diversity among marine aerobic anoxygenic phototrophs. *Nature*
480 415, 630–633. doi:10.1038/415630A

481 Bengtsson, M.M., Wagner, K., Schwab, C., Urich, T., Battin, T.J., 2018. Light availability impacts structure
482 and function of phototrophic stream biofilms across domains and trophic levels. *Molecular Ecology*
483 27, 2913–2925. doi:10.1111/MEC.14696

484 Berg, I.A., 2011. Ecological aspects of the distribution of different autotrophic CO₂ fixation pathways.
485 *Applied and Environmental Microbiology* 77, 1925–1936. doi:10.1128/AEM.02473-10

486 Blankinship, J.C., Niklaus, P.A., Hungate, B.A., 2011. A meta-analysis of responses of soil biota to global
487 change. *Oecologia* 165, 553–565. doi:10.1007/S00442-011-1909-0/TABLES/3

488 Boschker, H.T.S., Vasquez-Cardenas, D., Bolhuis, H., Moerdijk-Poortvliet, T.W.C., Moodley, L., 2014.
489 Chemoautotrophic carbon fixation rates and active bacterial communities in intertidal marine
490 sediments. *PLoS One* 9. doi:10.1371/JOURNAL.PONE.0101443

491 Bressan, M., Trinsoutrot Gattin, I., Desaire, S., Castel, L., Gangneux, C., Laval, K., 2015. A rapid flow
492 cytometry method to assess bacterial abundance in agricultural soil. *Applied Soil Ecology* 88, 60–
493 68. doi:10.1016/J.APSoIL.2014.12.007

494 Carey, C.C., Ibelings, B.W., Hoffmann, E.P., Hamilton, D.P., Brookes, J.D., 2012. Eco-physiological
495 adaptations that favour freshwater cyanobacteria in a changing climate. *Water Research* 46, 1394–
496 1407. doi:10.1016/J.WATRES.2011.12.016

497 Delarue, F., Laggoun-Défarge, F., Disnar, J.R., Lottier, N., Gogo, S., 2011. Organic matter sources and
498 decay assessment in a Sphagnum-dominated peatland (Le Forbonnet, Jura Mountains, France):
499 Impact of moisture conditions. *Biogeochemistry* 106, 39–52. doi:10.1007/S10533-010-9410-
500 0/FIGURES/5

501 Demeke, T., Eng, M., Holigroski, M., Lee, S.J., 2021. Effect of Amount of DNA on Digital PCR Assessment
502 of Genetically Engineered Canola and Soybean Events. *Food Analytical Methods* 14, 372–379.
503 doi:10.1007/S12161-020-01889-Y/TABLES/4

504 Du, H., Jiao, N., Hu, Y., Zeng, Y., 2006. Real-time PCR for quantification of aerobic anoxygenic
505 phototrophic bacteria based on *pufM* gene in marine environment. *Journal of Experimental Marine
506 Biology and Ecology* 329, 113–121. doi:10.1016/J.JEMBE.2005.08.009

507 Feng, Y., Lin, X., Mao, T., Zhu, J., 2011. Diversity of aerobic anoxygenic phototrophic bacteria in paddy
508 soil and their response to elevated atmospheric CO₂. *Microbial Biotechnology* 4, 74.
509 doi:10.1111/J.1751-7915.2010.00211.X

510 Frossard, A., Hammes, F., Gessner, M.O., 2016. Flow cytometric assessment of bacterial abundance in
511 soils, sediments and sludge. *Frontiers in Microbiology* 7, 195298.
512 doi:10.3389/FMICB.2016.00903/BIBTEX

513 Frostegård, A., Bååth, E., 1996. The use of phospholipid fatty acid analysis to estimate bacterial and
514 fungal biomass in soil. *Biology and Fertility of Soils* 22, 59–65. doi:10.1007/BF00384433

515 Ge, T., Wu, X., Chen, X., Yuan, H., Zou, Z., Li, B., Zhou, P., Liu, S., Tong, C., Brookes, P., Wu, J., 2013.
516 Microbial phototrophic fixation of atmospheric CO₂ in China subtropical upland and paddy soils.
517 *Geochimica et Cosmochimica Acta* 113, 70–78. doi:10.1016/J.GCA.2013.03.020

518 Gilbert, D., Amblard, C., Bourdier, G., Francez, A., 1998. The Microbial Loop at the Surface of a
519 Peatland:Structure, Function, and Impact of Nutrient Input. *Microbial Ecology* 35, 83–93.
520 doi:<https://doi.org/10.1007/s002489900062>

521 Gomez-Saez, G. V., Ristova, P.P., Sievert, S.M., Elvert, M., Hinrichs, K.U., Bühring, S.I., 2017. Relative
522 importance of chemoautotrophy for primary production in a light exposed marine shallow
523 hydrothermal system. *Frontiers in Microbiology* 8, 257720. doi:10.3389/FMICB.2017.00702/BIBTEX

524 Graham, E.D., Heidelberg, J.F., Tully, B.J., 2018. Potential for primary productivity in a globally-
525 distributed bacterial phototroph. *The ISME Journal* 12, 1861–1866. doi:10.1038/S41396-018-0091-
526 3

527 Guo, G., Kong, W., Liu, J., Zhao, J., Du, H., Zhang, X., Xia, P., 2015. Diversity and distribution of
528 autotrophic microbial community along environmental gradients in grassland soils on the Tibetan
529 Plateau. *Applied Microbiology and Biotechnology* 99, 8765–8776. doi:10.1007/S00253-015-6723-X

530 Hamard, S., Céréghino, R., Barret, M., Sytiuk, A., Lara, E., Dorrepaal, E., Kardol, P., Küttim, M.,
531 Lamentowicz, M., Leflaive, J., Le Roux, G., Tuittila, E.S., Jassey, V.E.J., 2021a. Contribution of
532 microbial photosynthesis to peatland carbon uptake along a latitudinal gradient. *Journal of Ecology*
533 109, 3424–3441. doi:10.1111/1365-2745.13732

534 Hamard, S., Küttim, M., Céréghino, R., Jassey, V.E.J., 2021b. Peatland microhabitat heterogeneity drives
535 phototrophic microbe distribution and photosynthetic activity. *Environmental Microbiology* 23,
536 6811–6827. doi:10.1111/1462-2920.15779

537 Hammes, F., Goldschmidt, F., Vital, M., Wang, Y., Egli, T., 2010. Measurement and interpretation of
538 microbial adenosine tri-phosphate (ATP) in aquatic environments. *Water Research* 44, 3915–3923.
539 doi:10.1016/J.WATRES.2010.04.015

540 Higuchi, R., Fockler, C., Dollinger, G., Watson, R., 1993. Kinetic PCR analysis: real-time monitoring of DNA
541 amplification reactions. *Bio/Technology* (Nature Publishing Company) 11, 1026–1030.
542 doi:10.1038/NBT0993-1026

543 Hindson, B.J., Ness, K.D., Masquelier, D.A., Belgrader, P., Heredia, N.J., Makarewicz, A.J., Bright, I.J.,
544 Lucero, M.Y., Hiddessen, A.L., Legler, T.C., Kitano, T.K., Hodel, M.R., Petersen, J.F., Wyatt, P.W.,
545 Steenblock, E.R., Shah, P.H., Bousse, L.J., Troup, C.B., Mellen, J.C., Wittmann, D.K., Erndt, N.G.,
546 Cauley, T.H., Koehler, R.T., So, A.P., Dube, S., Rose, K.A., Montesclaros, L., Wang, S., Stumbo, D.P.,
547 Hodges, S.P., Romine, S., Milanovich, F.P., White, H.E., Regan, J.F., Karlin-Neumann, G.A., Hindson,
548 C.M., Saxonov, S., Colston, B.W., 2011. High-throughput droplet digital PCR system for absolute
549 quantitation of DNA copy number. *Analytical Chemistry* 83, 8604–8610.
550 doi:10.1021/AC202028G/SUPPL_FILE/AC202028G_SI_001.PDF

551 Hou, Y., Chen, S., Zheng, Y., Zheng, X., Lin, J.M., 2023. Droplet-based digital PCR (ddPCR) and its
552 applications. *TrAC Trends in Analytical Chemistry* 158, 116897. doi:10.1016/J.TRAC.2022.116897

553 Huang, Q., Huang, Y., Wang, B., Dippold, M.A., Li, H., Li, N., Jia, P., Zhang, H., An, S., Kuzyakov, Y., 2022.
554 Metabolic pathways of CO₂ fixing microorganisms determined C-fixation rates in grassland soils
555 along the precipitation gradient. *Soil Biology and Biochemistry* 172, 108764.
556 doi:10.1016/J.SOILBIO.2022.108764

557 Hügler, M., Sievert, S.M., 2011. Beyond the Calvin cycle: autotrophic carbon fixation in the ocean.
558 *Annual Review of Marine Science* 3, 261–289. doi:10.1146/ANNUREV-MARINE-120709-142712

559 IPCC, 2023. Climate Change 2023: Synthesis Report. Contribution of Working Groups I, II and III to the
560 Sixth Assessment Report of the Intergovernmental Panel on Climate Change [Core Writing Team,
561 H. Lee and J. Romero (eds.)]. IPCC, Geneva, Switzerland, 184 pp., doi: 10.59327/IPCC/AR6-
562 9789291691647.

563 Jassey, V.E.J., Hamard, S., Lepère, C., Céréghino, R., Corbara, B., Küttim, M., Leflaive, J., Leroy, C., Carrias,
564 J.-F., 2022. Photosynthetic microorganisms effectively contribute to bryophyte CO₂ fixation in
565 boreal and tropical regions. *ISME Communications* 2022 2:1 2, 1–10. doi:10.1038/s43705-022-
566 00149-w

567 Jassey, V.E.J., Signarbieux, C., Hättenschwiler, S., Bragazza, L., Buttler, A., Delarue, F., Fournier, B.,
568 Gilbert, D., Laggoun-Défarge, F., Lara, E., T. E. Mills, R., Mitchell, E.A.D., Payne, R.J., Robroek,
569 B.J.M., 2015. An unexpected role for mixotrophs in the response of peatland carbon cycling to
570 climate warming. *Scientific Reports* 5, 1–10. doi:10.1038/srep16931

571 Karl, D.M., 1980. Cellular nucleotide measurements and applications in microbial ecology.
572 *Microbiological Reviews* 44, 739–796. doi:10.1128/MR.44.4.739-796.1980

573 Keselman, H.J., Rogan, J.C., 1977. The Tukey multiple comparison test: 1953–1976. *Psychological Bulletin*
574 84, 1050–1056. doi:10.1037/0033-2909.84.5.1050

575 Keshri, J., Yousuf, B., Mishra, A., Jha, B., 2015. The abundance of functional genes, cbbL, nifH, amoA and
576 apsA, and bacterial community structure of intertidal soil from Arabian Sea. *Microbiological*
577 *Research* 175, 57–66. doi:10.1016/J.MICRES.2015.02.007

578 Koblížek, M., Béjà, O., Bidigare, R.R., Christensen, S., Benitez-Nelson, B., Vetriani, C., Kolber, M.K.,
579 Falkowski, P.G., Kolber, Z.S., 2003. Isolation and characterization of *Erythrobacter* sp. strains from
580 the upper ocean. *Archives of Microbiology* 180, 327–338. doi:10.1007/S00203-003-0596-6

581 Kokkoris, V., Vukicevich, E., Richards, A., Thomsen, C., Hart, M.M., 2021. Challenges Using Droplet Digital
582 PCR for Environmental Samples. *Applied Microbiology* 1, 74–88.
583 doi:10.3390/APPLMICROBIOL1010007

584 Kusian, B., Bowien, B., 1997. Organization and regulation of *cbb* CO₂ assimilation genes in autotrophic
585 bacteria. *FEMS Microbiology Reviews* 21, 135–155. doi:10.1111/J.1574-6976.1997.TB00348.X

586 Le Geay, M., Lauga, B., Walcker, R., Jassey, V.E.J., 2024. A meta-analysis of peatland microbial diversity
587 and function responses to climate change. *Soil Biology and Biochemistry* 189, 109287.
588 doi:10.1016/J.SOILBIO.2023.109287

589 Lew, S., Lew, M., Koblížek, M., 2016. Influence of selected environmental factors on the abundance of
590 aerobic anoxygenic phototrophs in peat-bog lakes. *Environmental Science and Pollution Research*
591 23, 13853–13863. doi:10.1007/S11356-016-6521-8/TABLES/4

592 Liao, H., Hao, X., Qin, F., Delgado-Baquerizo, M., Liu, Y., Zhou, J., Cai, P., Chen, W., Huang, Q., 2023.
593 Microbial autotrophy explains large-scale soil CO₂ fixation. *Global Change Biology* 29, 231–242.
594 doi:10.1111/GCB.16452

595 Lin, X., Green, S., Tfaily, M.M., Prakash, O., Konstantinidis, K.T., Corbett, J.E., Chanton, J.P., Cooper, W.T.,
596 Kostka, J.E., 2012. Microbial community structure and activity linked to contrasting biogeochemical
597 gradients in bog and fen environments of the Glacial Lake Agassiz Peatland. *Applied and*
598 *Environmental Microbiology* 78, 7023–7031. doi:10.1128/AEM.01750-12

599 Liu, Z., Sun, Y., Zhang, Y., Feng, W., Lai, Z., Fa, K., Qin, S., 2018. Metagenomic and 13C tracing evidence
600 for autotrophic atmospheric carbon absorption in a semiarid desert. *Soil Biology and Biochemistry*
601 125, 156–166. doi:10.1016/J.SOILBIO.2018.07.012

602 Li, Yuqian, Ma, J., Yu, Y., Li, Yijia, Shen, X., Huo, S., Xia, X., 2022. Effects of multiple global change factors
603 on soil microbial richness, diversity and functional gene abundances: A meta-analysis. *Science of*
604 *The Total Environment* 815, 152737. doi:10.1016/J.SCITOTENV.2021.152737

605 Lode, E., Küttim, M., Kiivist, I.K., 2017. Indicative effects of climate change on groundwater levels in
606 estonian raised bogs over 50 years. *Mires and Peat* 19. doi:10.19189/MAP.2016.OMB.255

607 Mpamah, P.A., Taipale, S., Rissanen, A.J., Biasi, C., Nykänen, H.K., 2017. The impact of long-term water
608 level draw-down on microbial biomass: A comparative study from two peatland sites with different
609 nutrient status. *European Journal of Soil Biology* 80, 59–68. doi:10.1016/J.EJSOBI.2017.04.005

610 Mullis, K., Faloona, F., Scharf, S., Saiki, R., Horn, G., Erlich, H., 1986. Specific enzymatic amplification of
611 DNA in vitro: the polymerase chain reaction. *Cold Spring Harbor Symposia on Quantitative Biology*
612 51, 263–273. doi:10.1101/SQB.1986.051.01.032

613 Nakagawa, S., Takai, K., 2008. Deep-sea vent chemoautotrophs: diversity, biochemistry and ecological
614 significance. *FEMS Microbiology Ecology* 65, 1–14. doi:10.1111/J.1574-6941.2008.00502.X

615 Nichols, J.E., Peteet, D.M., 2019. Rapid expansion of northern peatlands and doubled estimate of carbon
616 storage. *Nature Geoscience* 12, 917–921. doi:10.1038/s41561-019-0454-z

617 Nowak, M.E., Beulig, F., Von Fischer, J., Muhr, J., Küsel, K., Trumbore, S.E., 2015. Autotrophic fixation of
618 geogenic CO₂ by microorganisms contributes to soil organic matter formation and alters isotope
619 signatures in a wetland mofette. *Biogeosciences* 12, 7169–7183. doi:10.5194/BG-12-7169-2015

620 Øvreås, L., Forney, L., Daae, F.L., Torsvik, V., 1997. Distribution of bacterioplankton in meromictic Lake
621 Sælevannet, as determined by denaturing gradient gel electrophoresis of PCR-amplified gene
622 fragments coding for 16S rRNA. *Applied and Environmental Microbiology* 63, 3367.
623 doi:10.1128/AEM.63.9.3367-3373.1997

624 Pearman, J.K., Biessy, L., Howarth, J.D., Vandergoes, M.J., Rees, A., Wood, S.A., 2022. Deciphering the
625 molecular signal from past and alive bacterial communities in aquatic sedimentary archives.
626 *Molecular Ecology Resources* 22, 877–890. doi:10.1111/1755-0998.13515

627 Pinheiro, L.B., Coleman, V.A., Hindson, C.M., Herrmann, J., Hindson, B.J., Bhat, S., Emslie, K.R., 2012.
628 Evaluation of a droplet digital polymerase chain reaction format for DNA copy number
629 quantification. *Analytical Chemistry* 84, 1003–1011.
630 doi:10.1021/AC202578X/SUPPL_FILE/AC202578X_SI_002.PDF

631 Qiu, C., Zhu, D., Ciais, P., Guenet, B., Peng, S., 2020. The role of northern peatlands in the global carbon
632 cycle for the 21st century. *Global Ecology and Biogeography* 29, 956–973. doi:10.1111/GEB.13081

633 Reczuga, M.K., Lamentowicz, M., Mulot, M., Mitchell, E.A.D., Buttler, A., Chojnicki, B., Słowiński, M.,
634 Binet, P., Chiapusio, G., Gilbert, D., Słowińska, S., Jassey, V.E.J., 2018. Predator–prey mass ratio
635 drives microbial activity under dry conditions in Sphagnum peatlands. *Ecology and Evolution* 8,
636 5752–5764. doi:10.1002/ECE3.4114

637 Rodríguez, A., Rodríguez, M., Córdoba, J.J., Andrade, M.J., 2015. Design of primers and probes for
638 quantitative real-time PCR methods. *Methods in Molecular Biology* 1275, 31–56. doi:10.1007/978-
639 1-4939-2365-6_3/COVER

640 Rowlands, V., Rutkowski, A.J., Meuser, E., Carr, T.H., Harrington, E.A., Barrett, J.C., 2019. Optimisation of
641 robust singleplex and multiplex droplet digital PCR assays for high confidence mutation detection
642 in circulating tumour DNA. *Scientific Reports* 9. doi:10.1038/S41598-019-49043-X

643 RStudio Team, 2020. RStudio: Integrated Development for R.

644 Sato-Takabe, Y., Hirose, S., Hori, T., Hanada, S., 2020. Abundance and Spatial Distribution of Aerobic
645 Anoxygenic Phototrophic Bacteria in Tama River, Japan. *Water* 12, 150. doi:10.3390/W12010150

646 Sato-Takabe, Y., Nakao, H., Kataoka, T., Yokokawa, T., Hamasaki, K., Ohta, K., Suzuki, S., 2016.
647 Abundance of Common Aerobic Anoxygenic Phototrophic Bacteria in a Coastal Aquaculture Area.
648 *Frontiers in Microbiology* 7. doi:10.3389/FMICB.2016.01996

649 Selesi, D., Pattis, I., Schmid, M., Kandeler, E., Hartmann, A., 2007. Quantification of bacterial RubisCO
650 genes in soils by *cbbL* targeted real-time PCR. *Journal of Microbiological Methods* 69, 497–503.
651 doi:10.1016/J.MIMET.2007.03.002

652 Shapiro, S.S., Wilk, M.B., 1965. An analysis of variance test for normality (complete samples). *Biometrika*
653 52, 591–611. doi:10.1093/BIOMET/52.3-4.591

654 Sherwood, A.R., Presting, G.G., 2007. Universal primers amplify a 23S rDNA plastid marker in Eukaryotic
655 algae and cyanobacteria. *Journal of Phycology* 43, 605–608. doi:10.1111/J.1529-
656 8817.2007.00341.X

657 Sidstedt, M., Jansson, L., Nilsson, E., Noppa, L., Forsman, M., Rådström, P., Hedman, J., 2015. Humic
658 substances cause fluorescence inhibition in real-time polymerase chain reaction. *Analytical
659 Biochemistry* 487, 30–37. doi:10.1016/J.AB.2015.07.002

660 Solomon, S., Qin, D., Manning, M., Chen, Z., Marquis, M., Averyt, K.B., Tignor, M., Millor, H.L., 2007.
661 Contribution of Working Group I to the Fourth Assessment Report of the Intergovernmental Panel
662 on Climate Change, 2007. Cambridge University Press, Cambridge, United Kingdom and New York,
663 NY, USA.

664 Strack, M., Davidson, S.J., Hirano, T., Dunn, C., 2022. The Potential of Peatlands as Nature-Based Climate
665 Solutions. *Current Climate Change Reports* 8, 71–82. doi:10.1007/s40641-022-00183-9

666 Sytiuk, A., Cérégino, R., Hamard, S., Delarue, F., Guittet, A., Barel, J.M., Dorrepaal, E., Küttim, M.,
667 Lamentowicz, M., Pourrut, B., Robroek, B.J.M., Tuittila, E.S., Jassey, V.E.J., 2022. Predicting the
668 structure and functions of peatland microbial communities from Sphagnum phylogeny, anatomical
669 and morphological traits and metabolites. *Journal of Ecology* 110, 80–96. doi:10.1111/1365-
670 2745.13728

671 Tang, K., Jia, L., Yuan, B., Yang, S., Li, H., Meng, J., Zeng, Y., Feng, F., 2018. Aerobic anoxygenic
672 phototrophic bacteria promote the development of biological soil crusts. *Frontiers in Microbiology*
673 9. doi:10.3389/FMICB.2018.02715

674 Tang, K., Liu, Y., Zeng, Y., Feng, F., Jin, K., Yuan, B., 2021. An Aerobic Anoxygenic Phototrophic Bacterium
675 Fixes CO₂ via the Calvin-Benson-Bassham Cycle. *BioRxiv* 2021.04.29.441244.
676 doi:10.1101/2021.04.29.441244

677 Taylor, S.C., Laperriere, G., Germain, H., 2017. Droplet Digital PCR versus qPCR for gene expression
678 analysis with low abundant targets: from variable nonsense to publication quality data. *Scientific
679 Reports* 7, 1–8. doi:10.1038/s41598-017-02217-x

680 Vogelstein, B., Kinzler, K.W., 1999. Digital PCR. *Proceedings of the National Academy of Sciences of the
681 United States of America* 96, 9236–9241. doi:10.1073/PNAS.96.16.9236

682 Wang, D., Wang, S., Du, X., He, Q., Liu, Y., Wang, Z., Feng, K., Li, Y., Deng, Y., 2022. ddPCR surpasses
683 classical qPCR technology in quantitating bacteria and fungi in the environment. *Molecular Ecology
684 Resources* 22, 2587–2598. doi:10.1111/1755-0998.13644

685 Wang, Xiaofan, Howe, S., Deng, F., Zhao, J., 2021. Current Applications of Absolute Bacterial
686 Quantification in Microbiome Studies and Decision-Making Regarding Different Biological
687 Questions. *Microorganisms* 9. doi:10.3390/MICROORGANISMS9091797

688 Wang, Xiayu, Li, W., Xiao, Y., Cheng, A., Shen, T., Zhu, M., Yu, L., 2021. Abundance and diversity of
689 carbon-fixing bacterial communities in karst wetland soil ecosystems. *CATENA* 204, 105418.
690 doi:10.1016/J.CATENA.2021.105418

691 Wang, Y., Huang, Y., Zeng, Q., Liu, D., An, S., 2023. Biogeographic distribution of autotrophic bacteria
692 was more affected by precipitation than by soil properties in an arid area. *Frontiers in Microbiology*
693 14, 1303469. doi:10.3389/FMICB.2023.1303469/BIBTEX

694 Wen, X., Unger, V., Jurasinski, G., Koebsch, F., Horn, F., Rehder, G., Sachs, T., Zak, D., Lischeid, G., Knorr,
695 K.H., Böttcher, M.E., Winkel, M., Bodelier, P.L.E., Liebner, S., 2018. Predominance of methanogens
696 over methanotrophs in rewetted fens characterized by high methane emissions. *Biogeosciences*
697 15, 6519–6536. doi:10.5194/BG-15-6519-2018

698 Wickham, H., 2016. *ggpolt2* Elegant Graphics for Data Analysis 211.

699 Witte, A.K., Mester, P., Fister, S., Witte, M., Schoder, D., Rossmanith, P., 2016. A Systematic Investigation
700 of Parameters Influencing Droplet Rain in the *Listeria monocytogenes* prfA Assay - Reduction of
701 Ambiguous Results in ddPCR. *PLOS ONE* 11, e0168179. doi:10.1371/JOURNAL.PONE.0168179

702 Xiao, K.Q., Bao, P., Bao, Q.L., Jia, Y., Huang, F.Y., Su, J.Q., Zhu, Y.G., 2014. Quantitative analyses of
703 ribulose-1,5-bisphosphate carboxylase/oxygenase (RubisCO) large-subunit genes (cbbL) in typical
704 paddy soils. *FEMS Microbiology Ecology* 87, 89–101. doi:10.1111/1574-6941.12193

705 Xue, J., Caton, K., Sherchan, S.P., 2018. Comparison of next-generation droplet digital PCR with
706 quantitative PCR for enumeration of *Naegleria fowleri* in environmental water and clinical samples.
707 *Letters in Applied Microbiology* 67, 322–328. doi:10.1111/LAM.13051

708 Xu, X., Thornton, P.E., Post, W.M., 2013. A global analysis of soil microbial biomass carbon, nitrogen and
709 phosphorus in terrestrial ecosystems. *Global Ecology and Biogeography* 22, 737–749.
710 doi:10.1111/GEB.12029

711 Xu, Z., Wang, S., Wang, Z., Dong, Y., Zhang, Y., Liu, S., Li, J., 2021. Effect of drainage on microbial enzyme
712 activities and communities dependent on depth in peatland soil. *Biogeochemistry* 155, 323–341.
713 doi:10.1007/S10533-021-00828-1/FIGURES/7

714 Yang, J., Kang, Y., Sakurai, K., Ohnishi, K., 2017. Fixation of carbon dioxide by chemoautotrophic bacteria
715 in grassland soil under dark conditions. *Acta Agriculturae Scandinavica, Section B — Soil & Plant*
716 *Science* 67, 362–371. doi:10.1080/09064710.2017.1281433

717 Yin, T., Qin, H. ling, Yan, C. rong, Liu, Q., He, W. qing, 2022. Low soil carbon saturation deficit limits the
718 abundance of cbbL-carrying bacteria under long-term no-tillage maize cultivation in northern
719 China. *Journal of Integrative Agriculture* 21, 2399–2412. doi:10.1016/S2095-3119(21)63800-5

720 Yuan, H., Ge, T., Chen, C., O'Donnell, A.G., Wu, J., 2012. Significant role for microbial autotrophy in the
721 sequestration of soil carbon. *Applied and Environmental Microbiology* 78, 2328–2336.
722 doi:10.1128/AEM.06881-11

723 Zhao, K., Zhang, B., Li, J., Li, B., Wu, Z., 2021. The autotrophic community across developmental stages of
724 biocrusts in the Gurbantunggut Desert. *Geoderma* 388, 114927.
725 doi:10.1016/J.GEODERMA.2021.114927

726 Zhao, Y., Xia, Q., Yin, Y., Wang, Z., 2016. Comparison of Droplet Digital PCR and Quantitative PCR Assays
727 for Quantitative Detection of *Xanthomonas citri* Subsp. *citri*. PLOS ONE 11, e0159004.
728 doi:10.1371/JOURNAL.PONE.0159004

729 Zhou, Z., Wang, C., Luo, Y., 2020. Meta-analysis of the impacts of global change factors on soil microbial
730 diversity and functionality. Nature Communications 11, 1–10. doi:10.1038/s41467-020-16881-7

731

732